PLOS ONE

RESEARCH ARTICLE

Effects of photosynthetic models on the calculation results of photosynthetic response parameters in young *Larix principis-rupprechtii* Mayr. plantation

Xuemei Ma[1,2], Qiang Liu[1]*, Zhidong Zhang[1], Zewen Zhang[1], Zeyu Zhou[1], Yu Jiang[1], Xuanrui Huang[1]*

1 College of Forestry, Hebei Agricultural University, Baoding Hebei, China, **2** Anyang Institute of Technology Anyang Henan, Anyang, China

* hxr1962@163.com (XRH); qiangliu2015@126.com (QL)

Citation: Ma X, Liu Q, Zhang Z, Zhang Z, Zhou Z, Jiang Y, et al. (2021) Effects of photosynthetic models on the calculation results of photosynthetic response parameters in young *Larix principis-rupprechtii* Mayr. plantation. PLoS ONE 16(12): e0261683. https://doi.org/10.1371/journal.pone.0261683

Editor: Dafeng Hui, Tennessee State University, UNITED STATES

Received: June 24, 2021

Accepted: December 7, 2021

Published: December 31, 2021

Data Availability Statement: All relevant data are within the manuscript and its Supporting Information files.

Funding: This research was funded by the Asia-Pacific Network for Sustainable Forest Management and Rehabilitation (APFNet) project (No.2021SP2-CHN), the National Science Foundation of China (No.32071795) and Talent Special Scientific Research Fund of Hebei Agricultural University (YJ201942).

Abstract

Accurately predicting the crown photosynthesis of trees is necessary for better understanding the C circle in terrestrial ecosystem. However, modeling crown for individual tree is still challenging with the complex crown structure and changeable environmental conditions. This study was conducted to explore model in modeling the photosynthesis light response curve of the tree crown of young *Larix principis-rupprechtii* Mayr. Plantation. The rectangular hyperbolic model (RHM), non-rectangular hyperbolic model (NRHM), exponential model (EM) and modified rectangular hyperbolic model (MRHM) were used to model the photosynthetic light response curves. The fitting accuracy of these models was tested by comparing determinants coefficients (R^2), mean square errors (*MSE*) and Akaike information criterion (*AIC*). The results showed that the mean value of R^2 of MRHM (R^2 = 0.9687) was the highest, whereas *MSE* value (*MSE* = 0.0748) and *AIC* value (*AIC* = -39.21) were the lowest. The order of fitting accuracy of the four models for P_n-*PAR* response curve was as follows: MRHM > EM > NRHM > RHM. In addition, the light saturation point (*LSP*) obtained by MRHM was slightly lower than the observed values, whereas the maximum net photosynthetic rates (P_{max}) modeled by the four models were close to the measured values. Therefore, MRHM was superior to other three models in describing the photosynthetic response curve, the accurate values were that the quantum efficiency (α), maximum net photosynthetic rate (P_{max}), light saturation point (*LSP*), light compensation point (*LCP*) and respiration rate (R_d) were 0.06, 6.06 μmol·m^{-2}s^{-1}, 802.68 μmol·m^{-2}s^{-1}, 10.76 μmol·m^{-2}s^{-1} and 0.60 μmol·m^{-2}s^{-1}. Moreover, the photosynthetic response parameters values among different layers were also significant. Our findings have critical implications for parameter calibration of photosynthetic models and thus robust prediction of photosynthetic response in forests.

Competing interests: The authors have declared that no competing interests exist.

Introduction

As the largest carbon flux in global carbon (C) cycling, photosynthesis can assimilate CO_2 from the atmosphere and thus dedicating to climate change mitigation. It plays a crucial role in the material cycle and energy flow of forest ecosystems [1–3]. In addition to the stage of leaf development and genetic constitution of plant, photosynthesis is also strongly affected by surrounding environmental conditions (e.g., light, leaf, CO_2 concentration, humidity and temperature etc.), during which intensity of light and its availability particularly determine the amount of C assimilated by photosynthesis [4–7]. For the trees, the canopy is the most direct part for photosynthesis to response to incoming solar irradiance. Therefore, better understanding the mechanism of crown leaf photosynthesis response to light availability is thus critical for maintaining forest productivity and management, in particular for dynamic simulation growth models and in parameterization of crown photosynthesis.

Light response curves (*P*n-*PAR* curves) describe the relationship between net photosynthetic rate (P_n) and photosynthetically active radiation (*PAR*), and provide information about the photosynthetic efficiency of plants (e.g. quantum yield, the maximum photosynthetic capacity, light compensation point and leaf radiation use efficiency of leaves) [8–10]. The simulation of *P*n-*PAR* curves are becoming increasingly important to study the photosynthetic response process of plants to the environment, and analyze the primary productivity of vegetation and forests [1, 11–13]. A series of photo-physiological core parameters, such as maximum net photosynthetic rate (P_{max}), apparent quantum yield (*AQY*), light-saturation point (*LSP*), light-compensation point (*LCP*), and dark respiration rate (R_d), can be used to assess the canopy photosynthetic rate and capacity of plants in different growth stage. To date, in order to investigate the response of net photosynthetic rate (P_n) to light intensity of different plants, many models, including the rectangular hyperbola model (RHM) [14, 15], the nonrectangular hyperbola model (NRHM) [16, 17], the exponential model (EM) [18, 19], and the modified rectangular hyperbola model (MRHM) [20], have been widely applied in modeling the photosynthetic light-response curve (P_n-*PAR* curve) [1, 12]. However, RHM, NRHM, and EM are very complex, some photo- and biochemical parameters (such as P_{max} and *LSP*) are subject to environmental conditions and cannot be calculated directly using these models when light intensity are above zero [21–24], and the fitted values of photosynthetic parameters were significantly different from the measured ones [20, 25]. In the contrary, owing to the addition of two adjusting factors (β and γ) into this model, which made the model highly advantageous in fitting the photo-inhibition and light saturation stages [20, 26], the MRHM can directly produce P_{max} and *LSP*, and overcome the limitation of above three models, the accuracy were higher and the results were suitable for fitting P_n-*PAR* curve and photosynthetic parameters under various environmental conditions [20, 24, 26, 27], it has been successfully applied in simulating light-response curves of many plants, such as *Keteleeria calcarea* [28], *Pinu stabulaeformis Carr*. [29], *Pinus koraiensis* [30], *Betula utilis* [31].

Larix principis-rupprechtii Mayr (*Larch*)., one of the main species of the total area of all plantations in Northern China, plays an important role in wood production, biodiversity protection, and forest ecological construction, due to its advantages of fast growth, strong adaptability, and high economic value. To the best of our knowledge, little attention has been paid to the application of a variety of dynamic crown photosynthetic light-response models in *Larch*, and the fitting effect and differences of light responses by these models remains unclear. Therefore, the determinant coefficients (R^2), mean square error (*MSE*), and Akaike information criterion (*AIC*) were used to evaluated the performance of four types of light-response models(such as RHM, NRHM, EM, and MRHM) in 16-years-old *Larch*. Planation. The objectives of the study were to select an optimal P_n-*PAR* curve model for fitting the P_n-*PAR* curves

of *Larch*, and to explore the relationships between the parameters of the optimal P_n-*PAR* curve model and leaf vertical positions. The results are helpful to further explore the spatial heterogeneity of carbon sequestration capacity of *Larch* needles in canopy, and provide a basis for accurately estimating photosynthetic physiological characteristics and the productivity of its plantation.

Materials and methods

Ethics statement

Conflicts of interest. The authors declare no conflict of interest.

Ethical approval. The authors declare that this article does not contain any research with humans or animal subjects.

Site description and sample tree selection

The experiments were conducted in the field at the the scientific research base of the State Forestry and Grassland Bureau established by Hebei Agricultural University, and the practice Base for postgraduate training of Forestry Master's Degree in Hebei Agricultural University. which is located in Saihanba Forest Farm of Weichang County of Hebei Province in the northern China (Fig 1, Table 1). The farm was mainly composed with *Larixprincipis-rupprechtii*, *Populusdavidiana*, *Betula platyphylla*, and *Quercus mongolica*. The total forest coverage is approximately 82.6%, including 72.6% plantation.

Three sample plots (20 m width × 30 m length) were set up within 16-year-old *Larch* plantations of the same habitat. The diameter at breast height (DBH, cm) and tree height (H, m) were measured for all trees with the D >5 cm in each plot, and the mean D (Dm) for three plots were calculated independently. Then, three sample trees, whose D values respectively was similar to Dm of the three plots, were selected to represent experimental materials. According to the previous studies, for trees, the upper limit of the P_n-*PAR* curves was significantly different within different crown whorls in the vertical direction [32–34]. Thus, we divided the crowns of three sample trees respectively into three vertical layers with the trisection of crown

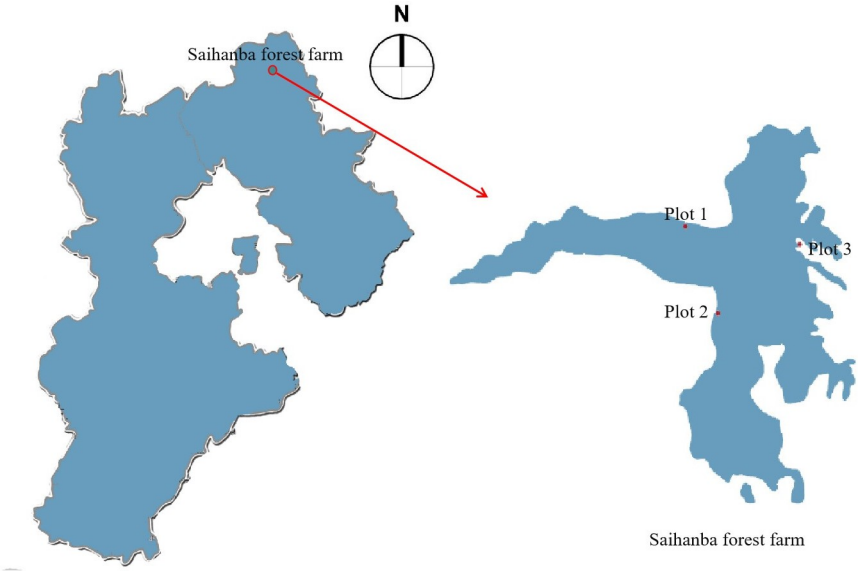

Fig 1. Study location and field experiment of *L. principis-rupprechtii* in Hebei Province, China.

https://doi.org/10.1371/journal.pone.0261683.g001

Table 1. Description of sample site used in the experiment.

Sample site	Latitude (N)	Longitude (E)	Elevation (m)	Climate	Annual mean temperature (˚C)	Annual precipitation (mm)	Annual evaporation (mm)	Sunshine hours (h_s)	Number of frost-free period (d)	Population size (hm^2)
Saihanba Forest Farm	42˚02′-42˚36′	116˚51′-117˚39	1500–2067	cold temperate semi-arid and semi humid continental monsoon	-1.5 (from -42.8 to 30.9˚C)	452.6	1230	2368	60	93333

https://doi.org/10.1371/journal.pone.0261683.t001

depth (the distance from the top of the tree to the base of its live crown, CD), and each layer was divided into two parts in horizontal direction (sunny and shaded) (**Fig 2**) [35].

Measurements of the light-response process

The light responses of photosynthesis were measured using a portable photosynthetic gas analysis system (LI-6400, LI-COR, Inc., Lincoln, Nebraska, USA) coupled with a standard red-blue light-emitting diode (LED) radiation source (85% red, emission peak at 655 nm + 15% blue, emission peak at 465 nm) (Li-6400-02B, LI-COR, Inc., Lincoln, NE, USA), photosynthetic active radiations (PAR) intensities were set at thirteen lever of 2000, 1500, 1200, 1000, 800, 600, 400, 200, 150, 100, 50, 25, and 0 μmol (photons) $m^{-2}s^{-1}$). Before measuring, the instrument was preheated and calibrated each time, these sample needles were kept for 10–20 min at a CO_2 concentration of 380 μmol (photons) m^{-2} s^{-1} and a *PAR* value of 1,400 μmol (photons) m^{-2} s^{-1} in the leaf chamber, which reach a steady state around the needles. Then, the sample needles were allowed to equilibrate to 20˚C conditions for a minimum time of 2 min and a maximum of 3 min before the data were logged during the measurement of the P_n-*PAR* curves. The measurements (experiments) were conducted from 8:30 a.m. to 16:30 p.m. on a cloud-free periods day, with an air temperature at 24–26˚C and a relative humidity at 30–40%, the fixed exposure time for each level of *PAR* was set at 2–3 min, these methods are described previously [32, 33]. The data for the P_n-*PAR* curves were measured once every half month during the growing season (approximately from 15th June to 10th August) in 2018 and 2019

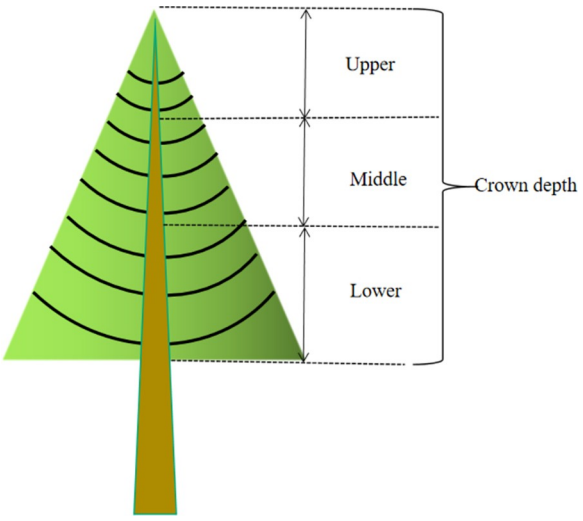

Fig 2. Sketch map of the crown divisions. Upper, Middle and Lower represent three equal divisions of crown depth in the vertical direction.

https://doi.org/10.1371/journal.pone.0261683.g002

Photosynthesis-light response curve-fitting model and its parameters

The rectangular hyperbola model, the nonrectangular hyperbola model, the exponential model, and the modified rectangular hyperbola model were used to fit the light-response curves and to estimate photosynthetic parameters. The environmental conditions (CO_2 concentration, temperature and humidity) are given. The expressions and parameters of the four models were as follows:

The rectangular hyperbola model (RHM) [15, 36] was represented to the following form:

$$P_n = \frac{\alpha I P_{max}}{\alpha I + P_{max}} - R_d \quad (1)$$

Where: P_n represents the net photosynthetic rate (μmol (photon) $m^{-2}{\cdot}s^{-1}$), a represents the initial quantum efficiency at low light intensities [22], P_{max} represents the maximum net photosynthetic rate (μmol (photon) $m^{-2}{\cdot}s^{-1}$), R_d represents the respiration rate in the dark (μmol (photon) $m^{-2}{\cdot}s^{-1}$), and I represents the *PAR*. α, P_{max}, and R_d are the main parameters to used describe the characteristics of the P_n-*PAR*. ***A*** is the initial slope of the P_n-*PAR* when *PAR* is 0--200 μmol$\cdot m^{-2}{\cdot}s^{-1}$, which indicates the plants' light use efficiency [37–39].

The P_{max} and *LSP* cannot be calculated directly using RHM, therefore, P_{max} was estimated and calculated by using the nonlinear least squares method under high light intensity [36, 40, 41], *LSP* could be expressed respectively as:

$$P_{max} = \boldsymbol{A} \times LSP - R_d \quad (2)$$

where: A (*AQE*) represents apparent quantum efficiency; *LSP* represents the light saturation point (μmol (photon) $m^{-2}{\cdot}s^{-1}$); R_d is as described above. A was obtained by fitting the light response data which *PAR* is equal to or less than 200 μmol (photon) $m^{-2}s^{-1}$)

$$LSP = (P_{max} + R_d)/\mathrm{A} \quad (3)$$

$$LCP = (R_d \times P_{max})/\alpha \times (P_{max} - R_d) \quad (4)$$

Where: *LCP* represents the light compensation point (μmol (photon) $m^{-2}{\cdot}s^{-1}$); *LSP*, A, P_{max}, R_d are as described above.

The nonrectangular hyperbola model (NRHM) [42] was represented to the following form:

$$P_n = \frac{\alpha I + P_{max} - \sqrt{(\alpha I + P_{max})^2 - 4\alpha\theta I P_{max}}}{2\theta} - R_d \quad (5)$$

where: P_n indicates the net photosynthetic rate (μmol (photon) $m^{-2}{\cdot}s^{-1}$); θ ($0 < \theta < 1$) indicates the convexity (curvilinear angle) (dimensionless); and α, I, $P_{max,}$ and R_d are as described above.

The *LSP* was calculated by. Formula 3.

The *LCP* can be obtained by:

$$LCP = \frac{(R_d \times P\mathrm{max} - \theta \times Rd^2)}{a \times (P\mathrm{max} - R\mathrm{d})} \quad (6)$$

Where: *LCP* represents the light compensation point (μmol (photon) $m^{-2}{\cdot}s^{-1}$); k, α, P_{max}, R_d are as described above.

The expressions for the exponential model (EM) [18] was represented to the following form:

$$P_n = P_{max} \cdot \left(1 - e^{\frac{-\alpha I}{P_{max}}}\right) - R_d \tag{7}$$

Where: e indicates the base of natural logarithm, α, I, $P_{\max}$, P_n, and R_d are as described above.

The *LSP* was calculated by. Formula 3,

The *LCP* was calculated by. Formula 8.

$$LCP = \frac{Pmax}{\alpha} \times ln\frac{Pmax}{P_{max} - R_d} \tag{8}$$

The modified rectangular hyperbola model (MRHM) [20, 23, 26] was represented to the following form:

$$P_n = \alpha \times \frac{1 - \beta I}{1 + \gamma I} I - R_d \tag{9}$$

where: β and γ are adjusting factors. β represents the photoinhibition item (dimensionless), γ represents the light saturation item (dimensionless), and $\gamma = \alpha/P_{\max}$. α, I, and R_d are as described above.

The $P_{\max}$, *LCP* and *LSP* were expressed on the modified rectangular hyperbola model in Eqs 10, 11, and 12, respectively:

$$P_{\max} = \alpha\left(\frac{\sqrt{\beta + \gamma} - \sqrt{\beta}}{\gamma}\right)^2 - R_d \tag{10}$$

$$LCP = \frac{R_d}{\alpha} \tag{11}$$

$$LSP = \frac{\sqrt{(\beta + \gamma)/\beta} - 1}{\gamma} \tag{12}$$

where *LCP*, *LSP*, α, β, γ, and R_d are as described above.

Model assessment and validation

The fitting quality of the different models were assessed by mean square errors (*MSE*), determinants coefficients (R^2), and Akaike information criterion (*AIC*), the best combination with the largest R^2 value and smallest *MSE* and *AIC* value represented the higher fitting accuracy.

Mean square error (*MSE*) was the average of squared forecast errors, it is the specific value of the sum of squared errors to the number of errors.

$$MSE = \frac{1}{n}\sum_{i=1}^{n}(y_i - \hat{y}_i)^2 \tag{13}$$

Determinants coefficients (R^2) represents the fitting degree of net photosynthetic rate and light intensity.

$$R^2 = 1 - \frac{\sum_{i=1}^{n}(y_i - \hat{y}_i)^2}{\sum_{i=1}^{n}(y_i - \bar{y}_i)^2} \tag{14}$$

Akaike information criterion (*AIC*) is a fined technique based on in-sample fit to estimate

the likelihood of a model to predict/estimate the future values.

$$AIC = 2k + nln\frac{\sum (y_i - \hat{y}_i)^2}{n} \quad (15)$$

where y_i, $\hat{y}_i$ and $\bar{y}_i$ in the equations above represented the measured value, the fitted value and the mean of the measured values, respectively n is the number of observations. k is the number of estimated parameters [43].

Statistical analyses

The measured light-response data are collated and analyzed and expressed as mean ± standard deviation (SD) of three replicates. Statistical analyses of the data were performed using two-way analysis of variance (ANOVA) by GraphPad Prism 8.0 or the SPSS software (version 18.0) and Duncan tests. Parameter values which are significantly different ($p<0.05$) are indicated by different letters.

Results

*P*n in response to *PAR*

To describe the relationships between P_n and *PAR*, photosynthetic light-response curves (P_n-*PARs*) of *Larch* was studied. The results showed that light response curves (P_n—*PAR*) fitted by NRHM, EM and MRHM from different layers were of similar tendency, while RHM were difficult to implement because the curves increased gradually with no extreme. Taking the middle layer as an example, the P_n-*PAR* curves could be divided into three stages, the net photosynthetic rate (P_n) increased linearly (rapidly) with the augments of photosynthetic available radiation (*PAR*) in the first stage, where $PAR < 200$ μmol (photon) m^{-2} s^{-1}, then increased nonlinearly up to the maximum P_n, in the second stage, the maximum P_n is 6.00 μmol (photons) $m^{-2}s^{-1}$ when *PAR* is 600 μmol (photons) $m^{-2}s^{-1}$, and decreased gradually with increasing *PAR* in the third stage (Fig 3). At the same *PAR*, needles under upper layer had a higher P_n than those of the middle and lower leaves, and P_n values under different leaf layer could be ranked as: Upper layer >Middle layer >lower layer.

Fitting and comparison of photosynthesis-light response curves

The fitting results showed the fitting P_n values of the four models were very close to the measured values actually when the *PAR* was low (*PAR* <100 μmol (photons) $m^{-2}s^{-1}$), the gap increased with an increasing *PAR*, and the difference in P_n was more remarkable. The P_n value simulated by NRHM, MRHM, and EM was slightly greater than measured value when *PAR* values are 200–2000 μmol (photons) $m^{-2}s^{-1}$, and the simulated pattern of P_n-*PAR* curves showed similar trend, the light-response curve was best described by three models, especially when light intensity (*PAR*) is beyond P_{max} (Fig 3). However, the P_n value simulated by the RHM increased with the increasing *PAR*, the fitting error was too large to use directly (Fig 3A1-3A3). In addition, the mean value of R^2 (range from 0.9748 to 0.9930) of the MRHM model was the highest among the four models, and *MSE* value (*MSE* range from 0.0646 to 0.0866 μmol (photons) m^{-2} s^{-1}) and *AIC* value (range from -45.7887 to -34.8321 respective) of the MRHM were significantly smaller than those of other three models in upper, middle and lower layer respectively (Table 2). In addition, MRHM model was superior to other three models in south and north orientation.

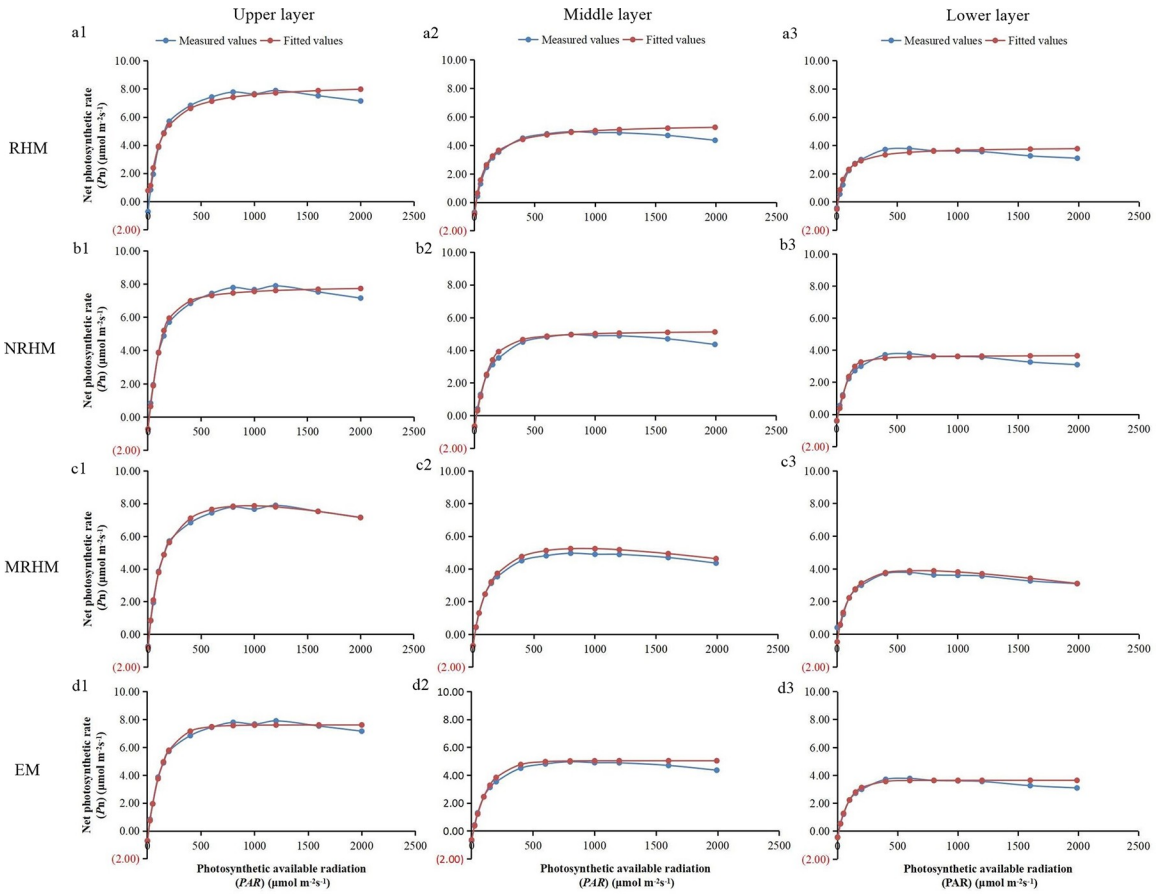

Fig 3. Comparison of the measured values and fitted values of net photosynthetic light response curves in different layers on the RHM (a1-a3), NRHM (b1-b3), MRHE (c1-c3) and EM (d1-d3) models. *PAR* represents photosynthetic available radiation, *MSE* represents mean square error, R^2 represents the coefficient of determination and *AIC* represents Akaike information criterion.

https://doi.org/10.1371/journal.pone.0261683.g003

Table 2. Fitting accuracy of different P_n-*PAR*.

Position	Fitting accuracy	P_n-*PAR* models			
		RHM	NRHM	MRHM	EM
Upper layer	*MSE*	0.2998	0.1903	0.0733	0.129
	R^2	0.967	0.982	0.993	0.9856
	AIC	-14.57	-17.18	-34.8321	-21.1756
Middle layer	*MSE*	0.23	0.1518	0.0646	0.144
	R^2	0.9628	0.9816	0.9923	0.9746
	AIC	-17.06	-20.79	-45.7887	-26.5774
Lower layer	*MSE*	0.4581	0.3	0.0866	0.2398
	R^2	0.8961	0.9473	0.9748	0.912
	AIC	-15.73	-19.27	-37.0383	-22.5198
North	*MSE*	0.3706	0.1988	0.0748	0.1565
	R^2	0.9563	0.9807	0.9904	0.9735
	AIC	-13.71	-17.52	-39.6365	-22.6997
South	*MSE*	0.288	0.2292	0.0748	0.1853
	R^2	0.9276	0.9598	0.983	0.9413
	AIC	-16.32	-20.38	-40.393	-22.943

https://doi.org/10.1371/journal.pone.0261683.t002

Fitting analysis of the photosynthetic parameters based on the models

The Fitting value of photosynthetic parameters were used to estimate the fitting quality of the model, its accuracy and rationality are affected by the model and layer [16, 19, 20, 27]. Therefore, it is very important to study the fitting effect of different models, different layers and different orientations on light response parameter of needle leaves. The results showed P_{max} calculated from the RHM, NRHM and EM were closer to the measured value in the up layer, and was slightly greater than the measured values in the middle and lower layer. The light saturation point (*LSP*) obtained by above three models were much lower than the measured values in the up, middle and lower layer respectively. The fitted values of P_{max} and *LSP* by MRHM were close to the measured values in each layer respectively. In addition, the *LSP* values were significant difference between MRHM and the other three models, while the P_{max} and *LCP* values were no significant difference, the *a* values of each model, which are the quantum efficiency at low irradiance, ranged from 0 to 0.125 [44], R_d value was closer among four models (Fig 4).

In the different layers, some simulated values of P_n-*PAR* response parameters revealed somewhat different, there was no significant difference for *LSP LCP* and R_d in upper and middle layers, but was significant difference in lower layers, the values of α and P_{max} were significant for in each layer. In addition, the layer is one of the main factors of affecting the light

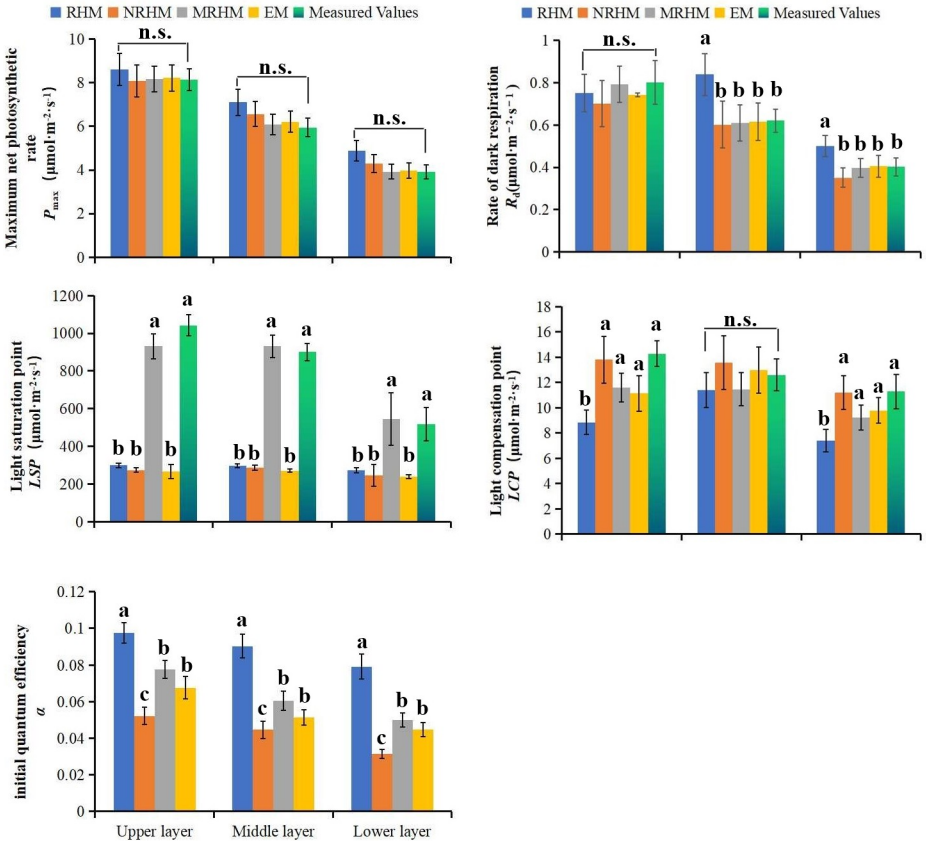

Fig 4. Comparison of light response parameters of different models at the same layer. (a) Parameters of (a) the initial quantum efficiency (*a*). (b) maximum net photosynthetic rate (P_{max}). (c) light saturation point (*LSP*). (d) light compensation point (*LCP*). (e) dark respiration rate (R_d) for needles at different models. different letters indicate significant difference at $p<0.05$ level with the least significant difference test, n.s. indicated no significant difference at the level of $P<0.05$.

https://doi.org/10.1371/journal.pone.0261683.g004

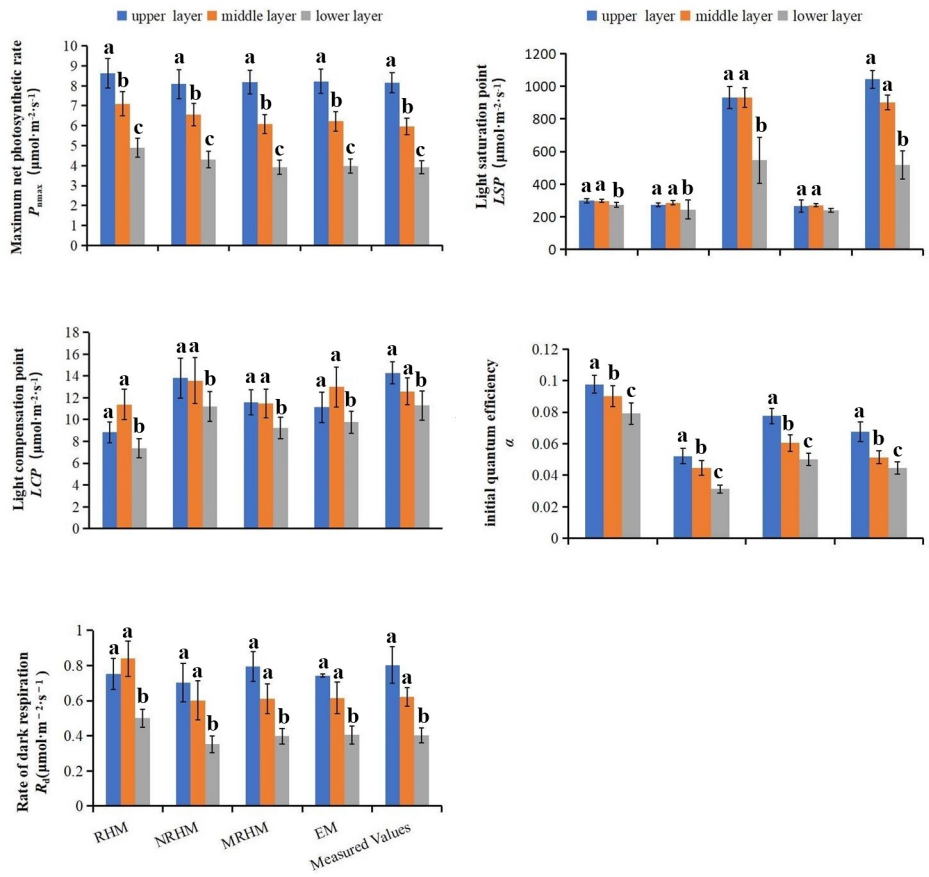

Fig 5. Comparison of light response parameters of different layers at the same model. (a) Parameters of the initial quantum efficiency (*a*). (b) maximum net photosynthetic rate (P_{max}). (c) light saturation point (*LSP*). (d) light compensation point(*LCP*). (e); dark respiration rate (R_d) for needles at different canyon (different letters indicate significant difference at $p<0.05$ level with the least significant difference test).

https://doi.org/10.1371/journal.pone.0261683.g005

response parameters (e.g. *a*, P_{max}, *LCP*) (Fig 4, S1 Table). Some simulated values of P_n-*PAR* response parameters calculated by MRHM was more accurate than those obtained from other three models (Fig 5, S1 Table). The photosynthetic parameters which were fitted by four models showed no significant difference between north and south direction (Fig 6, S3 Table).

Discussion

The light response curve (P_n-*PAR* curve) is an important tool for describing the response of the P_n to *PAR*, identifying a series of photosynthetic parameters and evaluating the photosynthetic efficiency of plants [11, 45, 46]. Therefore, constructing of P_n-*PAR* curve and choosing the appropriate model are helpful to simulate canopy photosynthesis and predict plant productivity [47, 48]. In the study, the net photosynthetic rate increased initially and then decreased gradually with the increase of *PAR* (Fig 3), which was consistent with the study of leaf P_n-*PAR* curves of some plants in different growth stages [49, 50]. The results indicated light energy absorbed by plants exceeded the needs of plants, the absorption of the excessive light energy would restricted photosynthetic mechanism and series of enzymatic reaction rates in the chloroplasts and result in photo-inhibition of *Larch*. The upper limit value of P_n-*PAR* curve maintained the state of upper layer >middle layer > lower layer during the whole growth period, which was also proved in other *Larch* species [32], indicated that the metabolic capacity was

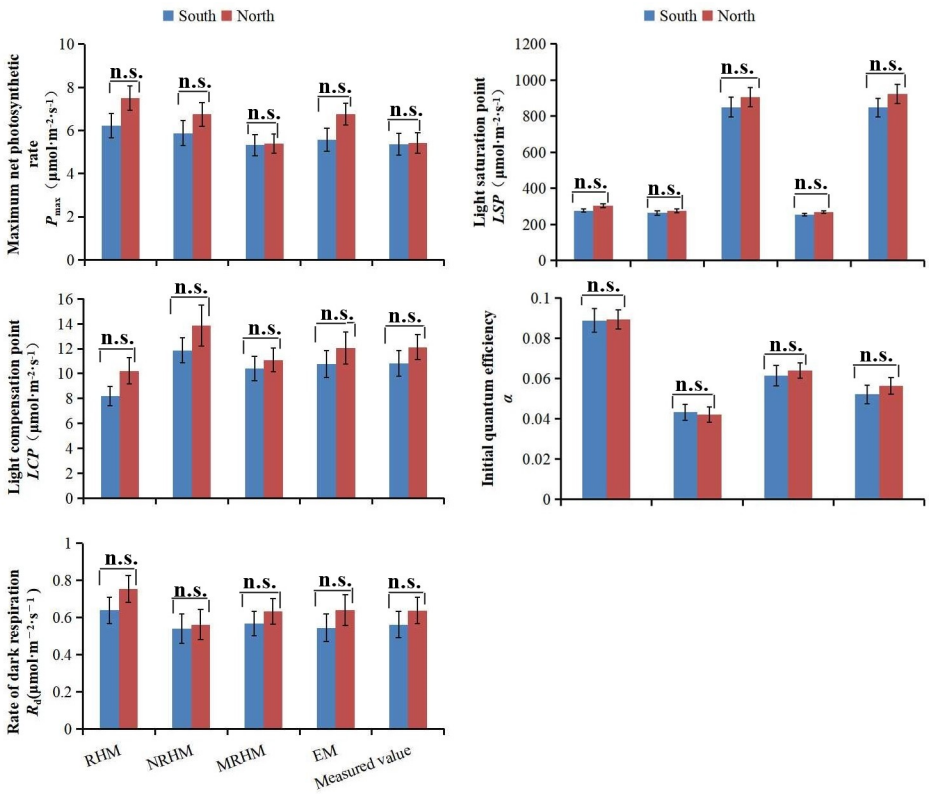

Fig 6. Comparison of light response parameters of different models between south and north direction. (a) maximum net photosynthetic rate (P_{max}); (b) dark respiration rate (R_d); (c) light saturation point (*LSP*). (d) light compensation point (*LCP*). (e) the initial quantum efficiency (α). (different letters indicate significant difference at $p<0.05$ level with the least significant difference test).

https://doi.org/10.1371/journal.pone.0261683.g006

closely related to the light environment [34]. The differences of the P_n-*PAR* curve among different canopies might be associated with leaf characteristics, solar elevation angle, higher chlorophyll a/b ratios, relative depth into crown (RDINC), etc [32, 51]. Additional, The photosynthetic parameters which were fitted by four models showed no significant difference between north and south direction, which was consistent with that of previous study [52].

The fitting of light-response model is an important method to describe the response mechanism of P_n to *PAR* and evaluate the photosynthetic efficiency [45]. Among four models, the P_n value simulated by the RHM consistently increased with the increasing *PAR* with no stable or declined trend (Fig 3A1–3A3), indicated that RHM was more suitable for fitting consistently increased type of P_n-*PAR* curves. This result agreed with the previous study [53]. Compared to the other three models, the determinants coefficients (R^2) value of the MRHM was the highest, and mean square errors (*MSE*) value and Akaike information criterion (*AIC*) value were the lowest (Table 2), indicated that MRHM performed better than other three models [23]. In addition, some fitted values of photosynthetic parameters (e.g P_{max} and *LSP*) were close to the measured values (Fig 4, S1 Table), Ye [20] has proved that the unique structure of MRHM made it more flexible in simulating different trends of P_n-*PAR* curves.

Compared with data fitted (Fig 3) and error analysis (Table 2) on the P_n-*PAR* curves of the needles at different leaf canopy, there was no significant difference for *LSP*, *LCP* and R_d in upper and middle layers, but was significant difference in lower layers. However, the values of *a* and P_{max} were significant in each layer. The P_n in the upper canopy was significantly higher

than those in the middle and lower canopy, which was not consistent with that of previous study [53]. The different may be due to the comprehensive effects of genetic diversity, different producing areas and environmental factors of trees [54]. It can be seen that layer was one of the main factors of affecting the light response parameters (e.g. *a*, P_{max}, *LCP*) (Fig 4, S1 Table).

Based on the above discussion, we considered that the light response process and photosynthetic parameter (P_{max}, *LSP*, *LCP*, and R_d) fitting by the MRHM models was more reliable (S2 Table). and MRHM could fit well the P_n-*PAR* curves of *Larch* (Fig 4, S2 Table). In addition, the P_n-*PAR* of the middle leaf layer can better reflect the changes in leaf layer photosynthetic parameters. However, the results, obtained in the vigorous growth period of *Larix principis rupprechtii* from June to August, are of spatial and temporal limitation in Saihanba, the further studies are needed to better understand the mechanisms of the photosynthetic physiological ecology of plants to the environment.

Conclusion

This study describe canopy photosynthesis for *Larix principis rupprechtii* plantation, the P_n-*PAR* curves and photosynthetic response parameters were measured under different layer of three planted *L. principis-rupprechtii* trees by different models during the growing season. The results showed that the fitting effect of MRHM model was superior to those of other three models and it could analyze the light-response data more accurately, the selection of the middle layer of the plant is the best when measuring the photosynthetic performance of the whole tree in combining with the analysis of fitting precision (Fig 3), the accurate values were as follows: α, P_{max}, *LSP*, *LCP* and R_d were 0.06, 6.08 μmol·$m^{-2}s^{-1}$, 931.08 μmol·$m^{-2}s^{-1}$, 11.45 μmol·$m^{-2}s^{-1}$ and 0.61 μmol·$m^{-2}s^{-1}$, respectively. This study not only helps to further explore the spatial heterogeneity of carbon sequestration capacity of *Larix principis rupprechtii* leaves in canopy, but also provides a scientific and effective guidance for accurately estimating the productivity of *Larix principis rupprechtii* plantation.

Supporting information

S1 Table. P_n-*PAR* response parameters of leaves in different layers of *Larch*. Black letter 'a' indicates significant differences between models, red letter 'a' indicates significant differences among different layers.
(DOC)

S2 Table. Analysis of light response parameters at different layers.
(DOC)

S3 Table. Analysis of light response parameters between south and north.
(DOC)

Acknowledgments

The authors are grateful to Saihanba Forest Farm of Weichang County of Hebei Province for providing the material.

Author Contributions

Conceptualization: Xuemei Ma, Xuanrui Huang.

Formal analysis: Zeyu Zhou, Yu Jiang.

Writing – original draft: Zewen Zhang.

Writing – review & editing: Qiang Liu, Zhidong Zhang.

References

1. Zhang XQ, Xu DY. Eco-physiological modelling of canopy photosynthesis and growth of a Chinese fir plantation. For. Ecol. Manag. 2003; 173: 201–211. https://doi.org/10.1016/S0378-1127(02)00015-4
2. Allen AP, Gillooly JF, Brown JH. Linking the global carbon cycle to individual metabolism. Funct. Ecol. 2005; 19: 202–213. https://doi.org/10.1111/j.1365-2435.2005.00952.x
3. Quan XK, Wang CK. Acclimation and adaptation of leaf photosynthesis, respiration and phenology to climate change: A 30-year Larix gmelinii common-garden experiment. For. Ecol. Manag. 2018; 411: 166–175. https://doi.org/10.1016/j.foreco.2018.01.024
4. Kull O, Kruijt B. Leaf photosynthetic light response: A mechanistic model for scaling photosynthesis to leaves and canopies. Funct. Ecol. 1998; 12: 767–777. https://doi.org/10.2307/2390464
5. Atkin OK, Scheurwater I, Pons TL. High thermal acclimation potential of both photosynthesis and respiration in two lowland *Plantago* species in contrast to an alpine congeneric. Glob. Chang. Biol. 2006; 12: 500–515. https://doi.org/10.1111/j.1365-2486.2006.01114.x
6. Campbell C, Atkinson L, Zaragoza-Castells J, Lundmark M, Atkin O, Hurry V. Acclimation of photosynthesis and respiration is asynchronous in response to changes in temperature regardless of plant functional group. New Phytol. 2007; 176: 375–389. https://doi.org/10.1111/j.1469-8137.2007.02183.x PMID: 17692077
7. Sage RF, Kubien DS. The temperature response of C_3, and C_4, photosynthesis. Plant Cell Environ. 2010; 30: 1086–1106. https://doi.org/10.1111/j.1365-3040.2007.01682.x PMID: 17661749
8. Akhkha A, Reid I. Clarke DD. Photosynthetic light response curves determined with the leaf oxygen electrode: minimisation of errors and signifcance. Planta. 2001; 214: 135–141. https://doi.org/10.1007/s004250100599 PMID: 11762163
9. Johnson GN, Murchie E. Gas exchange measurements for determination of photosynthetic efciency in Arabidopsis leaves. Methods Mol Biol. 2011; 775: 311–326. https://doi.org/10.1007/978-1-61779-237-3_17 PMID: 21863451
10. Lobo FA, de Barros MP, Dalmagro HJ, Dalmolin C. Fitting net photosynthetic light-response curves with Microsoft Excel-a critical look at the models. Photosynthetica. 2013; 51: 445–456. https://doi.org/10.1007/s11099-013-0045-y
11. Henley WJ, Measurement and interpretation of photosynthetic light-response curves in algae in the context of photoinhibition and diel changes. Journal of Phycology. 1993; 29: 729–739. https://doi.org/10.1111/j.0022-3646.1993.00729.x
12. Jin S, Zhou XF, Fan J. Modeling daily photosynthesis of nine major tree species in northeast China. Forest Ecol. Manag. 2003; 184: 125–140. https://doi.org/10.1016/S0378-1127(03)00205-6
13. Wilson KB, Baldocchi DD, Hanson PJ, Leaf age affects the seasonal pattern of photosynthetic capacity and net ecosystem exchange of carbon in a deciduous forest. Plant Cell Environ. 2011; 24: 571–583. https://doi.org/10.1046/j.0016-8025.2001.00706.x
14. Kubiske ME, Pregitzer KS. Effects of elevated CO_2 and light availability on the photosynthetic light response of trees of contrasting shade tolerance. Tree Physiol. 1996; 16: 351–358. https://doi.org/10.1093/treephys/16.3.351 PMID: 14871736
15. Luo YQ, Hui DF, Cheng WX, Coleman JS, Johnson DW, Sims DA. Canopy quantum yield in a mesocosm study. Agricultural and Forest Meteorology. 2000; 100(1); 35–48. https://doi.org/10.1016/S0168-1923(99)00085-4
16. Dias-Filho MB. Photosynthetic light response of the C4 grasses Brachiaria brizantha and B. humidicola under shade. Sci. Agr. 2002; 59(1): 65–68. https://doi.org/10.1590/S0103-90162002000100009
17. Moreno-Sotomayor A, Weiss A, Paparozzi ET, Arkebauer T.J. Stability of leaf anatomy and light response curves of field grown maize as a function of age and nitrogen status. Journal of Plant Physiology. 2002; 159(8): 819–826. https://doi.org/10.1078/0176-1617-00809
18. Bassman JH, Zwier JC. Gas exchange characteristics of Populus trichocarpa, Populus deltoides and Populus trichocarpa × P. deltoids clones. -Tree Physiol. 1991; 8(2): 145–159. https://doi.org/10.1093/treephys/8.2.145 PMID: 14972886
19. Rascher U, Liebig M, Luttge U. Evaluation of instant light-response curves of chlorophyll fluorescence parameters obtained with a portable chlorophyll fluorometer on site in the field. Plant Cell and Environment. 2000; 23: 1397–1405. https://doi.org/10.1046/j.1365-3040.2000.00650.x
20. Ye ZP. A new model for relationship between irradiance and the rate of photosynthesis in *Oryza sativa*. Photosynthetica. 2007; 45: 637–640. https://doi.org/10.1007/s11099-007-0110-5

21. Steele JH. Environmental control of photosynthesis in the sea. Limnol. Oceanogr. 1962; 7: 137–150. https://doi.org/10.4319/lo.1962.7.2.0137

22. Marshall B, Biscoe PV. A Model for C_3 leaves describing the dependence of net photosynthesis on irradiance. J. Exp. Bot. 1980; 31(1): 29–39. https://doi.org/10.1093/jxb/31.1.41

23. Ye ZP, Yu Q. Comparison of new and several classical models of photosynthesis in response to irradiance. J. Plant Ecol. 2008a; 32(6): 1356–1361. https://doi.org/10.3773/j.issn.1005-264x.2008.06.016

24. Ye ZP, Wang JL. Comparison and analysis of light-response models of plant photosynthesis. J. Jinggangshan Univ. (Sci.Technol.). 2009; 30(4): 9–13. https://doi.org/1673-4718(2009)04-0009-05

25. Chen ZY, Peng ZS, Yang J, Chen WY, Ou-Yang ZM. A mathematical model for describing light-response curves in Nicotiana tabacum L. Photosynthetica. 2011; 49(3): 467–471. https://doi.org/10.1007/s11099-011-0056-5

26. Ye ZP, Yu Q. A coupled model of stomatal conductance and photosynthesis for winter wheat. Photosynthetica 2008b; 46(4): 637–640. https://doi.org/10.1007/s11099-008-0110-0

27. Chen WY, Chen ZY, Luo FY, Peng ZS, Yu MQ. Comparison between modified exponential model and common models of light-response curve.—Chinese Journal of Plant Ecology, 2012; 36: 1277–1285. https://doi.org/10.3724/SP.J.1258.2012.01277

28. Chai SF, Tang JM, Yang X, Xie WL, Wei X, Jiang YS. Fitting analysis for 4 Photosynthesis light-response curve model of Keteleeriancalcarea. Journal of Guang xi Academy of Sciences. 2015; 31(4): 286–291. https://doi.org/10.13657/j.cnki.gxkxyxb.20151126.001

29. Zhu SZ. Modeling on the Photosynthetic light-response curve of Chinese Pine (Pinu stabulaeformis Carr.). Journal of Shanxi University (Nat. Sci. Ed.). 2016; 39(4): 184, 679–685. https://doi.org/10.13451/j.cnki.shanxi.univ(nat.sci.).2016.04.028

30. Zu YG, Wei XX, Yu JH. Li DW, Pang HH, Tong L. Responses in the physiology and biochemistry of Korean pine (*Pinus koraiensis*) under supplementary UV-B radiation. Photosynthetica. 2011; 49: 448–458. https://doi.org/10.1007/s11099-011-0057-4

31. Xu ZF, Hu TX, Zhang YB. Effects of experimental warming on phenology, growth and gas exchange of treeline birch (*Betula utilis*) saplings, Eastern Tibetan Plateau, China. European Journal of Forest Research. 2012; 131(3): 811–819.

32. Liu Q, Dong LH, Li FR, Xie LF. Spatial heterogeneity of canopy photosynthesis for *Larix olgensis*. Chin. J. Appl. Ecol. 2016; 27: 2789–2796. https://doi.org/10.13287/j.1001-9332.201609.008

33. Liu Q, Dong LH, Li FR. Modeling net CO2, assimilation (AN) within the crown of young planted Larix olgensis trees. Can. J. For. Res. 2018; 48(9): https://doi.org/1085-1098.10.1139/cjfr-2018-0151

34. Liu Q, Li FR. Spatial and seasonal variations of standardized photosynthetic parameters under different environmental conditions for young planted *Larix olgensis* Henry Trees. Forests. 2018; 9: 522. https://doi.org/10.3390/f9090522

35. Liu Q, Jia WW, Li FR. Determination of the most effective design for the measurement of photosynthetic light-response curves for planted *Larix olgensis* trees. Scientific Reports. 2020; 10: 11664. https://doi.org/10.1038/s41598-020-68429-w PMID: 32669616

36. Kyei-Boahen S, Lada R, Astatkie T, Gordon R, Caldwell, C. Photosynthetic response of carrots to varying irradiances. Photosynthetica. 2003; 41(2): 301–305. https://doi.org/10.1023/B:PHOT.0000011967.74465.cc

37. Cox PM, Huntingford C, Harding RJ. A canopy conductance and photosynthesis model for use in a GCM land surface scheme. J. Hydrol. (Amst.) 1998; 212-213(1–4): 79–94. https://doi.org/10.1016/S0022-1694(98)00203–0

38. Gardiner ES, Krauss KW. Photosynthetic light response of flooded cherrybark oak (Quercus pagoda) seedlings grown in two light regimes. Tree Physiol. 2001; 21: 1103–1111. https://doi.org/10.1093/treephys/21.15.1103 PMID: 11581017

39. Larocque GR. Coupling a detailed photosynthetic model with foliage distribution and light attenuation functions to compute daily gross photosynthesis in sugar maple (Acer Saccharum Marsh.) stands. Ecol. Modell. 2002; 148: 213–232, https://doi.org/10.1016/s0304-3800(01)00442-2

40. Peek MS, Russek-Cohen E, Wait DA, Forseth IN. Physiological response curve analysis using nonlinear mixed models. Oecologia. 2002; 132: 175–180. https://doi.org/10.1007/s00442-002-0954-0 PMID: 28547349

41. Posada JM, Lechowicz MJ, Kitajima K. Optimal photosynthetic use of light by tropical tree crowns achieved by adjustment of individual leaf angles and nitrogen content. Annals of Botany. 2009; 103; 795–805. https://doi.org/10.1093/aob/mcn265 PMID: 19151040

42. Thornley J. Mathematical Models in Plant Physiology. London: Academic Press. 1976; https://doi.org/331.10.1017/S0014479700007675

43. Zhang GY, Fang BS. A uniform design-based back propagation neural network model for amino acid composition and optimal pH in G/11 xylanase. J. Chem.Technol. Biotechnol. 2006; 81(7): 1185–1189. https://doi.org/10.1002/jctb.1510

44. Ma YJ, Cao ZZ, Li Y. Photosynthetic Characteristics of Lespedez a tomentosa and Influencing Factors. ACT A AGRESTIA SINICA. 2010; 18(2): 183–186. https://doi.org/10.3724/SP.J.1077.2010.01263

45. Wang HZ, Han L, Xu YL Niu JL, Yu J. Simulated photosynthetic responses of Populus euphratica during drought stress using light-response models. Acta Ecol. Sin. 2017; 37: 2315–2324. https://doi.org/10.5846/stxb201511242373

46. Zheng T, Chen J, He L, Arain MA, Thomas SC, Murphy JG, et al. Inverting the maximum carboxylation rate (Vcmax) from the sunlit leaf photosynthesis rate derived from measured light response curves at tower flux sites. Agric. Meteorol. 236: 48–66. https://doi.org/2017.10.1016/j.agrformet.2017.01.008

47. Yuan WP, Liu SG, Zhou GS, Zhou GY, Tieszen LL, Baldocch D, et al. Deriving a light use efficiency model from eddy covariance flux data for predicting daily gross primary production across biomes. Agric. Forest Meteorol. 2007; 143(3–4): 189–207. https://doi.org/10.1016/j.agrformet.2006.12.00

48. Pinto H, Powell JR, Sharwood RE, Tissue DT, Ghannoum O. Variations in nitrogen use efficiency reflect the biochemical subtype while variations in water use efficiency reflect the evolutionary lineage of C4 grasses at interglacial CO2. Plant Cell Environ. 2016; 39(3): 514–526. https://doi.org/10.1111/pce.12636 PMID: 26381794

49. Shang LQ, Chen H, Pan CD, Photosynthetic physiological characteristics of two main walnut cultivars in southern Xinjiang Basin at different growth stages. Chin. Agric. Sci. Bull. 2018; 485: 67–74. CNKI: SUN:ZNTB.0.2018-14-010.

50. Zhang N, Su X, Zhang XB, Yao X, Cheng T, Zhu Y, et al. Monitoring daily variation of leaf layer photosynthesis in rice using UAVbased multi-spectral imagery and a light response curve model. Agricultural and Forest Meteorology. 2020; 291(15): 1. https://doi.org/10.1016/j.agrformet.2020.108098

51. Lang Y, Wang M, Zhang GC, Zhao QK. Experimental and simulated light responses of photosynthesis in leaves of three species under different soil water conditions. Photosynthetica. 2013; 51: 370–378. https://doi.org/10.1007/s11099-013-0036-z

52. Zhang YQ, Gao SL, Wei XB, Shi WH, Ma Z, Su SH. Effects of photosynthetic models on the calculation results of photosynthetic response parameters in Sapindus mukorossi leaves. Journal of Beijing Forestry University. 2019; 41(4): 32–40. https://doi.org/10.13332/j.1000−1522.20180163

53. Huang LS, Han HR, Niu SK, Cheng XQ, Zhou WS. Spatial heterogeneity of canopy photosynthesis in *Larch* Plantations. Journal of Nanjing Forestry University. 2017; 41(2): 193–197. https://doi.org/10.3969/j.issn.1000-2006.2017.02.029

54. Di XY, Li XN, Wang QX, Wang MB. Genetic diversity of natural populations of Larix principis-rupprechtii in Shanxi Province, China. Biochemical Systematics and Ecology. 2014; 54: 71–77. https://doi.org/10.1016/j.bse.2013.12.035